Optimization of InAs/GaAs quantum-dot structures and application to 1.3-μm mode-locked laser diodes*

Li Mi-Feng(李密锋)[a], Ni Hai-Qiao(倪海桥)[a]†, Ding Ying(丁 颖)[b], Bajek David[b], Kong Liang[b], Cataluna Maria Ana[b], and Niu Zhi-Chuan(牛智川)[a]

[a] State Key Laboratory of Superlattices and Microstructures, Institute of Semiconductors, Chinese Academy of Sciences, Beijing 100083, China
[b] School of Engineering, Physics and Mathematics, University of Dundee, Dundee DD1 4HN, UK

(Received 13 June 2013; revised manuscript received 2 September 2013; published online 20 December 2013)

The self-assembled growth of InAs/GaAs quantum dots by molecular beam epitaxy is conducted by optimizing several growth parameters, using a one-step interruption method after island formation. The dependence of photoluminescence on areal quantum-dot density is systematically investigated as a function of InAs deposition, growth temperature and arsenic pressure. The results of this investigation along with time-resolved photoluminescence measurements show that the combination of a growth temperature of 490 °C, with a deposition rate of 0.02 ML/s, under an arsenic pressure of 1×10^{-6} Torr (1 Torr = 1.33322×10^{2} Pa), provides the best compromise between high density and the photoluminescence of quantum dot structure, with a radiative lifetime of 780 ps. The applicability of this 5-layer quantum dot structure to high-repetition-rate pulsed lasers is demonstrated with the fabrication and characterization of a monolithic InAs/GaAs quantum-dot passively mode-locked laser operating at nearly 1300 nm. Picosecond pulse generation is achieved from a two-section laser, with a ∼ 19.7-GHz repetition rate.

Keywords: InAs quantum dots, molecular beam epitaxy, mode-locked laser, short pulse

PACS: 78.67.Hc, 42.55.Px, 42.60.Fc, 81.10.–h **DOI:** 10.1088/1674-1056/23/2/027803

1. Introduction

Quantum dot (QD) materials have been shown to provide a number of advantages for the development of high-performance ultrafast semiconductor lasers.[1,2] For example, QD structures have demonstrated intrinsic ultrafast absorption recovery times and lower values of saturation fluence than their quantum-well counterparts.[3,4] When being incorporated into semiconductor saturable absorbers, QD structures are of importance for the development of high-repetition rate mode-locked laser diodes (MLLDs).[5] On the other hand, the self-assembled growth of QD materials allows significant flexibility in engineering the dot density, dot sizes, and their distribution,[6,7] thus enabling broad gain bandwidth/absorption and the development of spectrally versatile mode-locked laser diodes (MLLDs).[8] Recent work has demonstrated how growth parameters could be used to control and optimize the ultrafast characteristics of QD semiconductor saturable absorber mirrors (QD-SESAMs).[9] The characteristic low saturation fluence of the QD-SESAM is linked with the low density of states associated with QD material, and as such, it is relatively independent of the growth parameters as shown in the same study. On the one hand, the monolayer (ML) coverage (and associated QD areal density) was found to have a dominant effect on both the modulation depth and absorption recovery time.[9] The modulation depth was found to increase with the ML coverage. On the other hand, the slow component of the absorption recovery time significantly reduced from 533 ps to 8.8 ps when the ML coverage varied from 1.6 ML to 2.7 ML. It is important to emphasise that the passively or hybrid mode-locked semiconductor lasers generate pulses with durations on the order of a few ps (rather than fs), and it is the slow component of the absorption recovery time in the saturable absorber that determines the dynamic net gain window, which initiates and sustains pulse formation.

The architecture of typical passively MLLDs consists of a multi-section laser integrating both gain and absorber, which are therefore fabricated in the same structure. As a result, the optimization of QD structures for such devices has to take into account the fact that they will influence the characteristics of both sections simultaneously.

In this paper, we present the results of the optimization of QD epitaxial structures designed for an MLLD, as a function of InAs deposition, growth temperature, and As pressure. Using an optimized structure, a multi-section laser is subsequently fabricated, with successful demonstration of mode-locked operation at a repetition rate of nearly 20 GHz. A pre-

*Project supported by the Natural Science Foundation of Beijing, China (Grant No. 4112060), the Special Foundation for National Key Scientific Instrument, China (Grant No. 2012YQ140005), the Open Fund of High Power Laser Laboratory, China Academy of Engineering Physics (Grant No. 2013HEL03), the National Natural Science Foundation of China (Grant No. 61274125), the National Basic Research Program, China (Grant No. 2010CB327601), the State Key Laboratory on Integrated Optoelectronics Open Project, China (Grant No. 2011KFB002). Y. Ding was financially supported by a Marie Curie International Incoming Fellowship within the 7th European Community Framework Programme, and M. A. Cataluna by the financial support through a Royal Academy of Engineering/EPSRC Research Fellowship.

†Corresponding author. E-mail: nihq@semi.ac.cn

© 2014 Chinese Physical Society and IOP Publishing Ltd

vious report in the literature has demonstrated 20-GHz monolithic hybrid mode-locked QD laser emitting at around 1.3 μm, with 6-mW peak power and 7-ps pulse width.[10] In this paper, we demonstrate a 19.7-GHz monolithic passive QD-MLLD with peak powers up to 112 mW and 8-ps pulse duration, which can be used for 20 Gbits/s all-optical clock recovery and other datacom applications.

2. Experimental methods

The Stranski–Krastanov self-assembled growth of the QD structure was carried out using a Veeco Mod GEN II solid source molecular beam epitaxy (MBE) system. All the samples were grown with one-step interruption method, unless otherwise stated. Traditional periodic growth-interrupted method[11] should open and shut the In shutter many times during the growth of QDs for higher-quality layers. The method used in this paper reduces the frequency of closing and opening of In shutter to protect the MBE system against fatigue damage. As will be shown later in the paper, this method also results in a higher photoluminescence intensity.

The growth was monitored *in situ* by reflection high-energy electron diffraction (RHEED). The critical coverage (D) was taken at the steep rise of the reflected intensity, at the point when the streaky pattern of the two-dimensional wetting layer turned into a number of Bragg spots, corresponding to the formation of the three-dimensional (3D) QDs.[11] In our previous work, a modified two-step growth was carried out.[12] In the present paper, the growth of InAs was continuous in both two steps. The growth was only interrupted for 1 min with the As shutter kept open, after the deposition of D. After 3D growth, additional deposition of $x \cdot D$ was carried out, for the ripening of the QDs. The total deposition of InAs QDs therefore corresponds to $(D + x \cdot D)$.

The QD laser epitaxial structure was grown on an Si-doped GaAs (001) substrate, which was composed of five self-assembled QD active regions. Each of the InAs QD layers was capped by 5-nm $In_{0.15}Gas_{0.85}As$ strain-reducing layer to improve the optical quality of the QD and increase the emission wavelength.[13,14] Figure 1 shows a schematic diagram of the QD epitaxial structure. The total five InAs QD layers are buried in 295-nm GaAs, and are separated by 50-nm GaAs barriers. Next to the GaAs waveguide, a graded index-separating confinement heterostructure (GRIN-SCH) was grown to increase the carrier and light trapping efficiency.[15,16]

The sample morphology was characterized *ex situ* by a NanonaviEsweep S-II atomic force microscope (AFM) in contact mode. Photoluminescence (PL) spectra were acquired at room temperature, using a Nicolet FTIR760 Fourier transform spectrometer with a liquid-nitrogen-cooled Ge detector. The excitation light used for these static PL measurements was the 632.8-nm line from an He–Ne laser. The time-resolved PL was also evaluated for a subset of samples, which were excited by a pulsed semiconductor laser emitting at 640 nm, while the transient photoluminescence was captured with an InGaAs detector.

<table>
<tr><td colspan="2">GaAs 100 nm (P++ 2E19)</td></tr>
<tr><td colspan="2">GaAs 50 nm (P++ 1E19)</td></tr>
<tr><td colspan="2">$Al_{0.4-0}Ga_{0.6-1}As$ 150 nm (P++ 2E18)</td></tr>
<tr><td colspan="2">$Al_{0.4}Ga_{0.6}As$ 1.3 μm (P++ 1E18)</td></tr>
<tr><td colspan="2">$Al_{0.4}Ga_{0.6}As$ 0.2 μm (P+ 1E17−1E18)</td></tr>
<tr><td colspan="2">$Al_{0-0.4}Ga_{1-0.6}As$ 150 nm</td></tr>
<tr><td colspan="2">GaAs 45 nm</td></tr>
<tr><td colspan="2">$In_{0.15}Ga_{0.85}As$ 5 nm</td></tr>
<tr><td colspan="2">InAs QD</td></tr>
<tr><td rowspan="3">4 loops</td><td>GaAs 50 nm</td></tr>
<tr><td>$In_{0.15}Ga_{0.85}As$ 5 nm</td></tr>
<tr><td>InAs QD</td></tr>
<tr><td colspan="2">GaAs 50 nm</td></tr>
<tr><td colspan="2">$Al_{0.4-0}Ga_{0.6-1}As$ 150 nm</td></tr>
<tr><td colspan="2">$Al_{0.4}Ga_{0.6}As$ 0.4 μm (N++ 1E18)</td></tr>
<tr><td colspan="2">$Al_{0.4}Ga_{0.6}As$ 1.1 μm (N++ 3E18)</td></tr>
<tr><td colspan="2">$Al_{0-0.4}Ga_{1-0.6}As$ 150 nm (N++ 3E18)</td></tr>
<tr><td colspan="2">GaAs 300 nm (N++ 3E18)</td></tr>
<tr><td colspan="2">GaAs (100) N++ substrate</td></tr>
</table>

Fig. 1. Schematic diagram of the quantum dot epitaxial structure.

3. Results and discussion

3.1. Optimization of InAs QD structures

The growth parameters of InAs deposition, growth temperature, and As pressure were investigated, with a view to obtain the best conditions to grow a high QD density sample, with a high PL intensity.

Firstly, various samples with different depositions of InAs were grown, at a fixed growth temperature of 500 °C and an As pressure of 1×10^{-6} Torr (1 Torr = 1.33322×10^{2} Pa). The growth rate is 0.02 ML/s. Figure 2 shows the PL intensity and density of the InAs QDs each as a function of the fraction of deposition of InAs (x), after the formation of QDs. When x is increased from 17% to 48%, the PL intensity first increases and goes up to a maximum when x value is 38%, and then decreases with x value further increasing.

A compromise x value (34%) was then chosen and kept constant, to further optimize the growth temperature. This corresponds to a monolayer coverage of 2.5 ML (indeed, the critical deposition is $\sim$ 1.86 ML, and an additional amount of 0.64 ML (1.865 ML$\times$0.34) was deposited after the formation of the QDs). For this InAs deposition value, InAs QD structures were grown at several different temperatures, ranging from 480 °C to 510 °C. The obtained PL intensity, density

of InAs QDs, and AFM images are shown in Fig. 3. The density increases when growth temperature decreases, which is consistent with the results in Refs. [17]–[19]. This can be explained by the fact that the surface migration of InAs is weakened at low growth temperature.[20] However, the PL intensity dramatically decreases for growth temperatures at or below 480 °C, even though the QD density is very high. This may be caused by dislocations or other defects formed at very low growth temperatures, and in fact, the growth mechanism could even deviate from the typical characteristics of the classical Stranski–Krastanov growth in this case. Moreover, and as depicted in the AFM image of the sample grown at 480 °C, the sizes of QDs are both inhomogeneous and smaller than those of the QDs grown at and above 490 °C, which also affects the PL intensity. For higher growth temperatures, the density decreases significantly with the increase of temperature, due to the increasingly high surface migration and desorption of In. Taking into account the effects on both PL intensity and density, are latively low growth temperature of 490 °C is therefore selected to grow the QD layers.

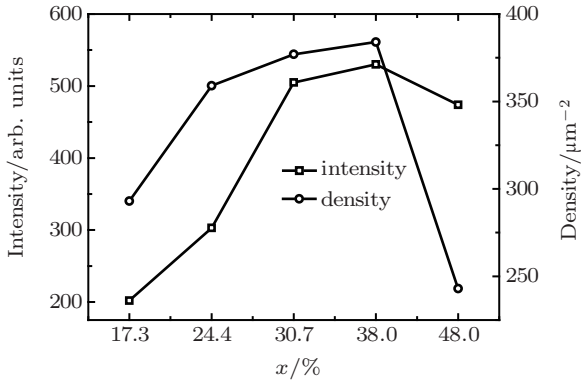


Fig. 2. Dependences of the PL intensity and QD density deposition of InAs on the fraction of deposition of InAs (x). The total deposition of InAs is $(1+x)\cdot D$. The growth temperature is 500 °C and the As pressure is 1×10^{-6} Torr.

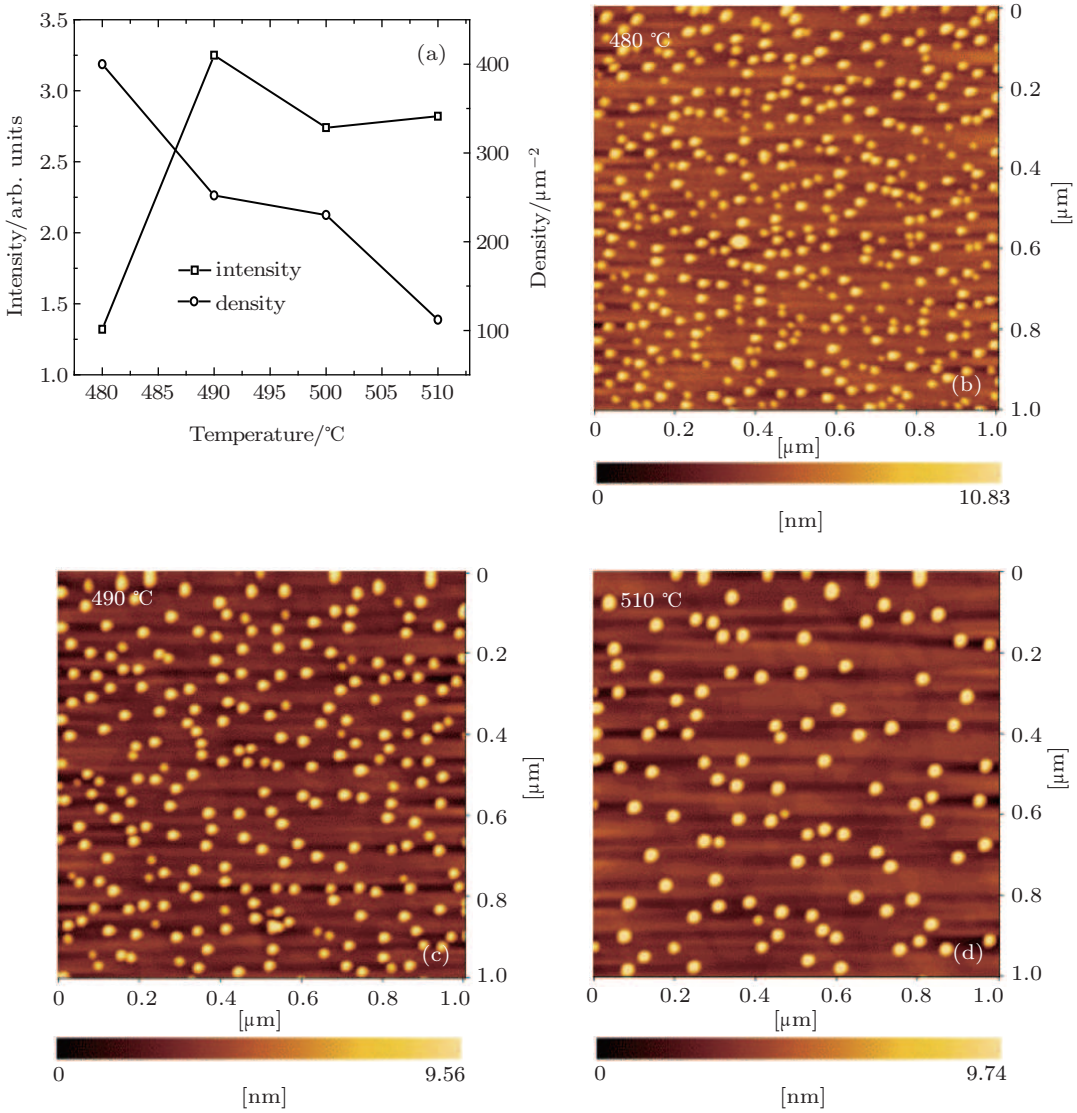


Fig. 3. (color online) Results obtained for an InAs deposition of 1.34D, at a growth rate of 0.02 ML/s and an As pressure of 1×10^{-6} Torr, under several growth temperatures. (a) Dependence of the dot density and PL intensity on growth temperature. (b)–(d) AFM scans of the samples grown at 480 °C, 490 °C, and 510 °C, respectively.

While keeping the temperature growth at 490 °C with growth rate 0.01 ML/s, a range of values of arsenic flux were investigated, at pressures ranging from 1×10^{-7} Torr to 3×10^{-6} Torr. The obtained results are shown in Fig. 4. The typical QD diameter and height were found to be 37 nm and 8 nm, respectively (Fig. 4(c)). From a comparison between Figs. 4(c) and 4(d), it becomes apparent that when the As pressure is lower than 1×10^{-6} Torr, the density of InAs QDs decreases, while the average size increases because of the surface migration enhancement.[19] When As fluxes are too high, clusters appear as shown in Fig. 4(b), while the PL intensity also decreases because of the lower density of InAs QDs. Nucleation cannot form under too low As fluxes as shown in Fig. 4(f), and QD islands are not detected. The highest density achieved is obtained to be $\sim5\times10^{10}$ cm^{-2}/sheet, when the As pressure is $\sim1\times10^{-6}$ Torr.

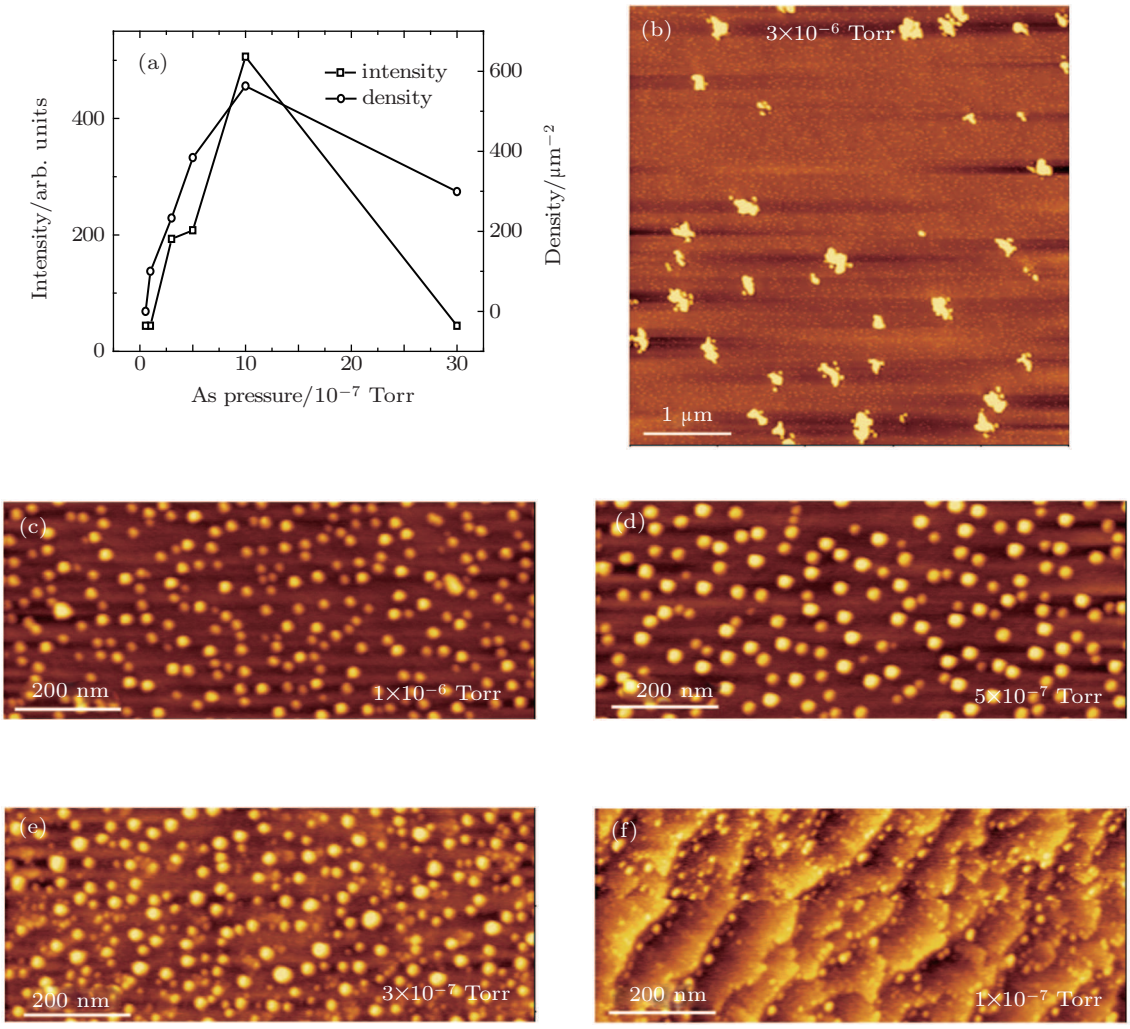


Fig. 4. (color online) (a) Dependences of PL and density each versus As pressure, and AFM images of InAs QDs at As pressures of (b) 3×10^{-6} Torr, (c) 1×10^{-6} Torr, (d) 5×10^{-7} Torr, (e) 3×10^{-7} Torr, (f) 1×10^{-7} Torr.

Table 1. Radiative lifetimes in InAs/GaAs quantum dots, corresponding to the ground state transition. Samples 1, 2, and 3 correspond to the results represented in Fig. 3.

Sample	Temperature/°C	Radiative lifetime/ps
1	500	1166
2	490	780
3	480	410

The lifetime of the radiative ground-state transition was subsequently characterized using time-resolved photoluminescence for a subset of samples corresponding to those depicted in Fig. 3. The radiative lifetimes of the QDs grown with different depositions and As pressures are similar. On the other hand, the radiative lifetime increases when the growth temperature increases, as shown in Table 1.

The lower radiative lifetime of sample 3 (which has the highest density of QDs and the lowest PL intensity) may be attributed to a higher concentration of defects which act as centers of non-radiative recombination. The previous study on the optimization of fast QD-SESAMs[9] showed that the sample with the highest QD density also displayed the fastest absorption recovery time, which the authors also attributed to the ex-

istence of non-radiative centers of recombination. One could infer from these results that there could be a possibility that sample 3 would also display the fastest absorption recovery time, among these three samples, which would be beneficial to a fast saturable absorber. However, it would not be feasible to select this structure for fabricating a multi-section MLLD, for the output power generated in the gain section would be too low due to the very poor luminescence performance of this wafer. For this reason, the sample 2 was chosen for the MLLD, for presenting the best compromise among radiative lifetime, PL intensity, and QD density.

The typical PL curves of this optimized InAs/GaAs QD structure at room temperature are shown in Fig. 5, for both one-step and periodic growth-interrupted method (at a growth temperature of 490 °C, growth rate of 0.02 ML/s, under an As pressure of 1×10^{-6} Torr). The emission wavelength is $\sim$ 1300 nm. The full width at half maximum (FWHM) is 41 meV and 30 meV for one-step and periodic growth-interrupted method, respectively. This difference can be attributed to a much longer interruption time for the periodic growth-interrupted method, which affords enough migration of InAs to form uniform QDs, leading to a narrower distribution of QD sizes and therefore a smaller FWHM. However, the high PL intensity and high density of QDs achievable by one-step interruption method are preferable for the fabrication of an MLLD, for affording higher output power levels and a broader gain/absorption bandwidth, which are of relevance to the generation of ultrashort pulses.

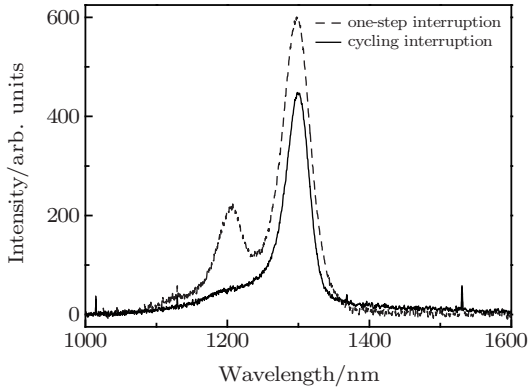


Fig. 5. Typical PL of the optimized InAs/GaAs QD structure, grown by two different methods: one-step or cycling interruption.

3.2. Fabrication and characterization of the InAs/GaAs QD-MLLD

The fabricated device had a 20-μm-wide optical ridge-waveguide, comprising an 1800-μm long gain section and a 300-μm long saturable absorber section. The top layer was etched to form a 50-μm gap separating the two sections, in order to isolate these electrically. The total length amounts to an overall 2.1 mm, corresponding to a pulse repetition rate of around $\sim$ 20 GHz. The fabrication process comprised standard photolithography and chemical wet etching steps. Both of the laser facets were uncoated. The laser was mounted p-side up on a copper heat sink using In solder, which is controlled at an operating temperature of 5 °C using a Peltier cooler.

The experimental setup used for MLLD characterization is presented in Fig. 6. The pulse duration was measured by a collinear autocorrelator. The mode-locking performance was further investigated with an RF spectrum analyzer in combination with a high-speed 29-GHz photodiode. An optical spectrum analyser was used to investigate the optical spectral characteristics.

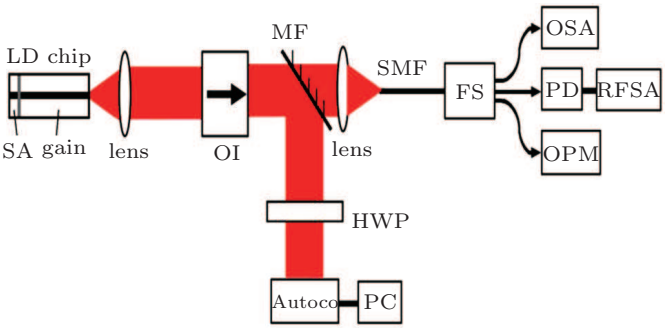


Fig. 6. (color online) Experimental setup. LD chip: laser diode chip; SA: saturable absorber; OI: optical isolator; HWP: half-wave plate; MF: mirror flipper; SMF: single-mode fiber; FS: fiber splitter; OSA: optical spectrum analyzer; Autoco: autocorrelator; PC: personal computer; PD: photo detector; RFSA: RF spectrum analyzer; OPM: fiber optical power meter.

The light-current characteristics of the QD lasers were measured with a reverse bias voltage applied to the saturable absorber (from 0 V to 6 V), as shown in Fig. 7. The central operating wavelength is $\sim$ 1300 nm. Hysteresis is clearly observed when a reverse bias voltage is applied to the absorber section, and becomes more pronounced with the increasing of reverse bias.

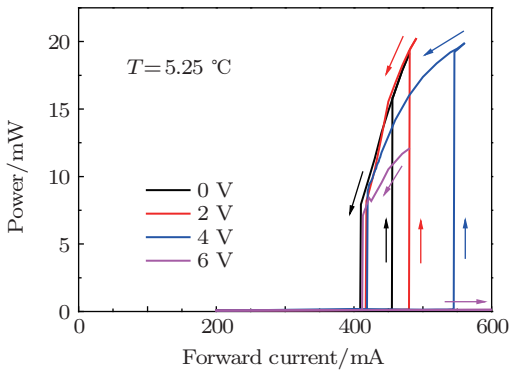


Fig. 7. (color online) *P–I* curves of MLLD for various reverse bias values.

Stable mode locking is observed for reverse bias values ranging from 2.7 V to 5.7 V. A peak power of 112 mW (89.9 mW) per facet is measured for a driving current of 470 mA and 2.7 V (5.7 V) reverse bias. The typical autocorrelation, RF, and optical spectra are shown in Fig. 8. For a

reverse bias of 5.7 V, a 19.66-GHz repetition rate is achieved. A sech^2-shaped pulse has been assumed to calculate the pulse duration which is 7.3 ps. In combination with a spectral bandwidth of 2.2 nm, this results in a time-bandwidth product of ~ 2.87. The generated pulse is therefore not transform-limited, and could be post-compressed in order to increase the peak power.

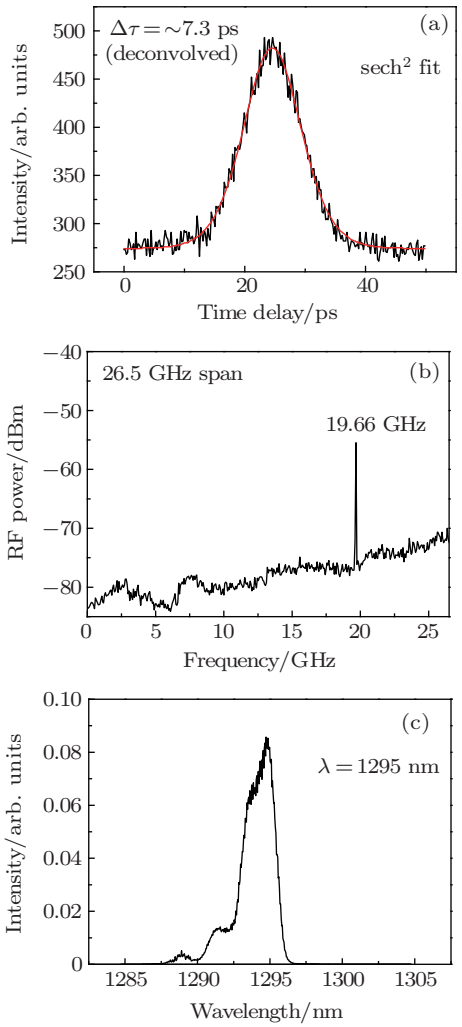


Fig. 8. (color online) (a) Autocorrelation, (b) RF spectrum, (c) optical spectrum for a reverse bias voltage of 5.7 V and a gain current of 470 mA.

It is important to add that despite the fact that only five QD layers are present in the active region, the laser emission always took place in the ground-state band. Moreover, the mirror reflectivities were not optimal: in the future, the back facet near the absorber could be made highly-reflective and the front facet could have a lower reflectivity coating, which would increase the output power.

4. Conclusion

Using one-step interruption method, the MBE growth of self-assembled InAs/GaAs QDs is optimized. The low operation frequencies of the shutter provide the opportunity for stable and highly efficient QD growth compared with the case using the traditional cycling interruption method. The PL and density of QDs are investigated to obtain the best growth parameters. Considering the PL intensity, density of QDs, and radiative lifetime, the parameters chosen to grow the five InAs/GaAs QDs active layers are a growth temperature of 490 °C, an InAs deposition fraction of 34%, under an As pressure of 1×10^{-6} Torr. Two-section monolithic QD-MLLDs are fabricated on the optimized structure and are successfully mode-locked. A stable train at a $\sim$ 20-GHz repetition rate is demonstrated. For a reverse bias voltage of 2.7 V (5.7 V), a peak power of 112 mW (89.9 mW) per facet is achieved, with a pulse duration of 8 ps (7.3 ps).

References

[1] Rafailov E U, Cataluna M A and Sibbett W 2007 *Nat. Photon.* **1** 395

[2] Rafailov E U, Cataluna M A and Avrutin E A 2011 *Ultrafast Lasers Based on Quantum Dot Structures: Physics and Devices* (Weinheim: Wiley-VCH) p. 272

[3] Borri P, Schneider S, Langbein W and Bimberg D 2006 *J. Opt. A: Pure Appl. Opt.* 833

[4] Li X, Feng D H, He H Y, Jia T Q, Shan L F, Sun Z R and Xu Z Z 2012 *Acta Phys. Sin.* **61** 197801 (in Chinese)

[5] Thompson M G, Rae A R, Xia M, Penty R V and White I H 2009 *IEEE J. Sel. Top. Quant.* **15** 661

[6] Tang N Y, Chen X S and Lu W 2005 *Acta Phys. Sin.* **54** 5855 (in Chinese)

[7] Solomon G S, Trezza J A and Harris J S 1995 *Appl. Phys. Lett.* **66** 3161

[8] Cataluna M, Ding Y, Nikitichev D I, Fedorova K A and Rafailov E U 2011 *IEEE J. Sel. Top. Quant.* **17** 1302

[9] Maas D, Bellancourt A, Hoffmann M, Rudin B, Barbarin Y, Golling M, Südmeyer T and Keller U 2008 *Opt. Express* **16** 18646

[10] Kuntz M, Fiol G, Lammlin M, Bimberg D, Thompson M, Tan K, Marinelli C, Penty R, White I and Ustinov V 2004 *Appl. Phys. Lett.* **85** 843

[11] Patella F, Fanfoni M, Arciprete F, Nufris S, Placidi E and Balzarotti A 2001 *Appl. Phys. Lett.* **78** 320

[12] Huang S S, Niu Z C, Zhan F, Ni H Q, Zhao H, Wu D H and Sun Z 2008 *Chin. Phys. B* **17** 323

[13] Tian P, Huang L R, Fei S P, Yu Y, Pan B, Xu W and Huang D X 2010 *Acta Phys. Sin.* **59** 5738 (in Chinese)

[14] Nishi K, Saito H, Sugou S and Lee J S 1999 *Appl. Phys. Lett.* **74** 1111

[15] Zhang Z, Wang Z, Xu B, Jin P, Sun Z and Liu F 2004 *IEEE Photon. Tech. Lett.* **16** 27

[16] Polland H J, Leo K, Rother K, Ploog K, Feldmann J, Peter G, Göbel E, Fujiwara K, Nakayama T and Ohta Y 1988 *Phys. Rev. B* **38** 7635

[17] Nakata Y, Mukai K, Sugawara M, Ohtsubo K, Ishikawa H and Yokoyama N 2000 *J. Cryst. Growth* **208** 93

[18] Garcia A, Mateo C, Defensor M, Salvador A, Hui H, Boothroyd C and Philpott E 2007 *J. Appl. Phys.* **102** 073526

[19] Chu L, Arzberger M, Bohm G and Abstreiter G 1999 *J. Appl. Phys.* **85** 2355

[20] Yamaguchi K, Yujobo K and Kaizu T 2000 *Jpn. J. Appl. Phys.* **39** 1245